Atmos. Chem. Phys. Discuss., 9, 12597–12614, 2009
www.atmos-chem-phys-discuss.net/9/12597/2009/

Atmospheric Chemistry and Physics Discussions

This discussion paper is/has been under review for the journal *Atmospheric Chemistry and Physics (ACP)*. Please refer to the corresponding final paper in *ACP* if available.

Variability of residence time in the Tropical Tropopause Layer during Northern Hemisphere winter

K. Krüger[1], **S. Tegtmeier**[2], **and M. Rex**[3]

[1]Leibniz-Institute for Marine Sciences at Kiel University (IFM-GEOMAR), Kiel, Germany
[2]Environment Canada, Toronto, Canada
[3]Alfred Wegener Institute for Polar and Marine Research, Potsdam, Germany

Received: 18 April 2009 – Accepted: 15 May 2009 – Published: 28 May 2009

Correspondence to: K. Krüger (kkrueger@ifm-geomar.de)

Published by Copernicus Publications on behalf of the European Geosciences Union.

Abstract

For the first time the long-term interannual and spatial variability of residence time (τ) is presented for the TTL between 360 K and 400 K theta (~14 to 18 km altitude). The analysis is based on a Lagrangian approach using offline calculated diabatic heating rates as vertical velocities, covering Northern Hemisphere (NH) winters from 1962–2004.

The residence time varies spatially. τ, analysed for the Lagrangian Cold Point (LCP), displays a longer duration time of air parcels between LCP and 400 K over the maritime continent (>50 days), as the LCP tropopause has a minimum over the maritime continent (<370 K theta). Comparing three theta layers within the TTL reveals the vertical dependence of τ. We derive a mean duration time of 34 days for 360–380 K (lower TTL), 38 days for 380–400 K (upper TTL) and 70 days for 360–400 K theta layers for the 1962–2001 period. A case analysis reveals, that τ is positively skewed for 360–380 K and 380–400 K during La Niña and El Niño Southern Oscillation (ENSO) neutral years. For these cases, ~60% of air parcels travel from 360 K to 380 K within 25 days. There is large interannual variability for τ varying up to ±20% from the long-term mean, with strongest variability seen in the lower part of the TTL. The interannual variability is influenced by extratropical and subtropical wave driving. Statistical analysis reveals a significant anti-correlation between the residence time and the extratropical and subtropical wave driving in the lowermost stratosphere.

1 Introduction

In recent years the relevance of natural halogenated source gases and primarily the relevance of marine produced very short lived substances (VSLS) has raised up research interests due to their large potential for depleting stratospheric ozone, if they reach the stratospheric overworld fast enough (<30 days) (WMO, 2007). The main source region of oceanic VSLS like bromocarbon are located in the tropical oceans

ACPD

9, 12597–12614, 2009

especially in upwelling regions close to the coast (Quack and Wallace, 2003). In the atmosphere, the tropical tropopause layer (TTL) is the main entrance region for trace gases travelling from the troposphere into the stratospheric overworld, where especially the maritime continent during NH winter season plays a dominant role (e.g. Holton and Gettelman et al., 2001). Transport through the TTL primarily arises as large-scale horizontal and slow (weeks to months) vertical processes accompanied by localized rapid (hours) convective overshooting. In this respect the transport time scale of large scale, slow ascent versus meso-scale, rapid overshooting in the TTL, limits the supply of halogens to the stratosphere and hence the stratospheric ozone depletion in mid-latitudes (WMO, 2007). In this study we are particularly interested in the large-scale, slow transport processes in the upper part of the TTL, which are primarily driven by diabatic radiative heating generated by the eddy driven residual circulation in the stratosphere (Dunkerton, 1978; Haynes et al., 1991).

Krüger et al. (2008) (hereafter K08) applied a Lagrangian approach to calculate long-term air mass transport through the TTL using offline calculated diabatic heating rates to overcome the known problems of using the noisy and strong vertical velocities of assimilation systems. K08 showed that the geographical distribution of the LCP is very robust and does not seem to be much affected by using the more realistic method with heating rates (alternative approach) compared to the vertical wind method (conventional approach). However, K08 found that differences in the density of trajectories, the distribution of diabatic ascent and in the residence time are all large. For the NH winters 2000–2001 and 2001–2002, they computed an average residence time of ~40 days between the LCP and 400 K for the alternative approach and only ~20 days for the conventional method. Both values lie within the uncertainty range of 20 and 80 days for the 360 K to 380 K layer summarized by WMO (2007), which is agreement with recent observational estimates for case studies (e.g. Park et al., 2007; Marcy et al., 2007). So far, we are not aware of any other study investigating the long-term interannual and spatial variability of residence time in the TTL.

ACPD
9, 12597–12614, 2009

The current paper will use the method and data described in K08, presenting the interannual and spatial variability of residence time for the TTL layer between the 360 K and 400 K theta levels during NH winter. The questions of how fast, where and when these TTL transport time scales occur will be addressed within this study.

2 Model and method

For calculating the inter-annual variability of residence time in the upper part of the TTL during the cold season (NH winter), we are using operational analyses of the European Centre for Medium Range Weather Forecast (opECMWF) (Simmons et al., 2005) and 40-years of ECMWF reanalyses (ERA40) (Uppala et al., 2005). Due to data availability, our Lagrangian analysis has been carried out for the period 1962–1963 to 2004–2005.

In contrast to previous TTL studies, a different approach is used to better constrain the vertical velocities in isentropic trajectory models of this region of the atmosphere: we apply a reverse domain filling trajectory model coupled with a radiative transfer model to calculate diabatic heating rates, that are used as vertical velocities. The model and the method employed are described in detail in K08 and Tegtmeier et al (2008). The advantage of using diabatic heating rates in the upper part of the TTL is demonstrated for a tropical campaign in the accompanying paper by Immler et al. (2007). The backward trajectories are initialized on a 2°×2° grid from 30° S to 30° N on the 400 K isentropic level for the period from December to February (DJF). This gives a total number N of 5580 trajectories per period. As we are only interested in the troposphere to stratosphere transport of air masses, the backward trajectories are required to pass the isentropic level of 360 K. To derive the residence time τ (days) from Lagrangian studies, the duration (Δt) the trajectories spend within a given theta layer ($\Delta\Theta$, in K), is sampled. The Lagragian diabatic heating Q_L (K/day) is directly related to τ as it gives the vertical velocity in $\Delta\Theta$ per Δt. The residence time is computed along each trajectory as the average between LCP and 400 K ($\tau_{\mathrm{LCP-400\,K}}$), 380 K and 400 K ($\tau_{\mathrm{380\,K-400\,K}}$), 360 K and 400 K ($\tau_{\mathrm{360\,K-400\,K}}$) and the layer between 360 K and 380 K

ACPD
9, 12597–12614, 2009

($\tau_{360\,K-380\,K}$). For this purpose, the duration time is calculated during the first crossing point of the requested theta layer. The climatology maps of τ show averages of trajectories inside a 5°×5° box. Only grid boxes sampled by trajectories are shown. Tropical averages are calculated between 30° S and 30° N. The density (ν) of the trajectories is given by $\nu = n/(N\,ny)$, where n is the number of trajectories sampled inside a grid box and ny is the number of years.

3 Results

3.1 Spatial variability of residence time

For a better comparison with our companion study (K08), tropical maps of residence time for the TTL layer between LCP and 400 K are shown for different time periods (Fig. 1). The duration time and the amount of water vapour within air parcels during the TTL passage determine the chemical processes and life time of VSLS reaching the stratosphere. The long-term DJF mean from 1962–2001 displays the maximum residence time of more than 50 days over the maritime continent, due to the fact that the LCP reaches its minimum tropopause height of less than 370 K over this region. This leads, perhaps unexpectedly, to the longest τ between LCP and 400 K. A secondary smaller maximum of 50 days is displaced northeast of Brazil, where again the LCP tropopause minimizes at 380 K. On the right side of Fig. 1, the zonal mean $\tilde{\tau}_{\mathrm{LCP-400\,K}}$ is compared with $\tilde{\tau}$ for fixed theta layers. $\tilde{\tau}_{\mathrm{LCP-400\,K}}$ shows a distinct meridional shape of residence time mirroring the meridional distribution of the LCP tropopause, which has its maximum $\tilde{\tau}_{\mathrm{LCP-400\,K}}$ (minimum $Q_{\mathrm{LCP-400\,K}}$, not shown here) over the Equator with decreasing (increasing) values towards the subtropics. For a better quantification of the residence time of air parcels within the TTL, we display $\tilde{\tau}$ for three different theta layers in the TTL (Fig. 1, right side). The shape of $\tilde{\tau}$ for fixed theta layers changes considerably. $\tilde{\tau}_{380\,\mathrm{K}-400\,\mathrm{K}}$ has a minimum of 35 days north of the Equator towards the NH winter hemisphere and a maximum of 41 days south of the Equator during the 1962–2001

ACPD
9, 12597–12614, 2009

DJF period. According to this, $\tilde{Q}_{380\,\mathrm{K}-400\,\mathrm{K}}$ has its maximum upwelling (0.65 K/day) north of the Equator (not shown), probably influenced by the enhanced eddy driven circulation towards the active winter stratosphere (K08). This meridional pattern vanishes for the $\tilde{\tau}_{360\,\mathrm{K}-380\,\mathrm{K}}$ and $\tilde{\tau}_{360\,\mathrm{K}-400\,\mathrm{K}}$ layers, indicating a more pronounced tropospheric influence for the this part of the TTL. $\tilde{\tau}_{360\,\mathrm{K}-380\,\mathrm{K}}$ and $\tilde{\tau}_{360\,\mathrm{K}-400\,\mathrm{K}}$ have tropical averages of 34 and 70 days respectively, whereas $\tau_{360\,\mathrm{K}-380\,\mathrm{K}}$ can reach below 25 days over the tropical Pacific.

The other two time periods (Fig. 1, middle and lower panel) reflect the contradictory results shown previously by (K08). Even though the DJF period 1991–2001 was colder than 1962–2001 (Fig. 3 in K08), less tropical upwelling occurred, which is in agreement with weaker wave driving observed during the cold NH winters in the early to mid 1990s (Pawson and Naujokat, 1999). This leads to a longer residence time over parts of the Indonesian islands (>60 days), although the LCP theta layer lies higher compared to 1962–2001, reflecting the complex influence of LCP temperature, height and Q on τ. The lower panel of Fig. 1 illustrates the 5-year mean of opECMWF data during the early 2000s, which has a smaller area of maximum $\tau_{\mathrm{LCP}-400\,\mathrm{K}}$ of 50 days over the maritime continent, although the LCP theta layer has a minimum Θ with largest extension. Inspecting $\tilde{Q}_{\mathrm{LCP}-400\,\mathrm{K}}$ (not shown) reveals that the strongest diabatic heating of 0.7 K/day occurs within this time period, maximizing just north of the Equator, which is also present in $\tilde{Q}_{380\,\mathrm{K}-400\,\mathrm{K}}$. This higher $\tilde{Q}$ leads to a shorter $\tilde{\tau}_{380\,\mathrm{K}-400\,\mathrm{K}}$ in the same region (Fig. 1, right side). Tropical averaging τ ($\hat{\tau}$) for the 380–400 K layer gives 37 days for 1962–2001, increasing to 38 days for 1992–2001 and decreasing to 36 days for the 2000–2004 DJF period. However, changes of $\hat{\tau}_{360\,\mathrm{K}-380\,\mathrm{K}}$ and $\hat{\tau}_{360\,\mathrm{K}-400\,\mathrm{K}}$ for the different time periods are not coherent with $\hat{\tau}$ for the upper TTL, indicating the presence of another influence possibly from the troposphere. The tropical averages for $\hat{\tau}_{360\,\mathrm{K}-380\,\mathrm{K}}/\hat{\tau}_{360\,\mathrm{K}-400\,\mathrm{K}}$ systematically decreases from 36/69 days for 1962–2001, to 32/69 days for 1992–2001 and 26/60 days for the 2000–2004 DJF period. The maximum density of LCP trajectories, located over the warm pool (K08 and Fig. 1), coincides with regions of $\tau_{360\,\mathrm{K}-380\,\mathrm{K}}$<25 days (not shown here). This indicates, that a large

ACPD
9, 12597–12614, 2009

amount of air parcels reaches 380 K, which is approximately the height of the LCP (Fig. 1), within the TTL in less than 25 days during NH winter.

3.2 Statistical distribution of residence time: a case study

For the rest of this study we concentrate on fixed theta layers, avoiding the dependence of τ_{LCP} on the LCP height. For a better understanding of the spatial and temporal variability, Fig. 2 presents the probability density function (PDF) of τ for given theta layers, concentrating on years with different ENSO phases. ENSO shows a clear spatial variation of LCP temperature and density distribution (Bonazzola and Haynes, 2004; Fueglistaler and Haynes, 2005; K08). The PDF residence time is sampled within 5-day bins centered at 0, 5, 10,. . ., 90 days. Thus, averaging the PDF residence time for one specific winter from Fig. 2 can give slightly different values compared to the winter averages derived from the synoptic maps (Fig. 1, see Sect. 2). $\tau_{380\,\mathrm{K}-400\,\mathrm{K}}$ for the ENSO neutral year 2001–2002 (red bars in Fig. 2a) displays a maximum peak of 0.27 (27%) probability at 20 days with a positive skew towards longer τ reaching up to 75 days (0.01 probability). The temporal average of τ ($\bar{\tau}$, calculated from the PDF) has a duration time of 34 days for air parcels travelling from 380 K to 400 K. The theta layer between 360 K to 380 K (blue filled bars) displays a maximum of 15 days (0.14 probability) with a shorter right tail reaching up to 65 days. $\bar{\tau}_{360\,\mathrm{K}-380\,\mathrm{K}}$ gives 28 days, a faster residence time than for the TTL layer above. Note that the average τ derived from the PDF in Fig. 2 is the τ derived from the Lagrangian histories of the air masses. This differs from τ that could be determined from averaging ascent rates at grid points in an Eulerian way, which would not reflect the real τ for the traveling air masses. It also differs slightly from values that would be derived from averaging over all geographical boxes shown in Fig. 1, because these Eulerian boxes do not contribute with even weight to the fully Lagrangian average shown here. The grey bars show τ between 360 K and 400 K θ layers, having an almost uniform distribution, indicating the influence of independent tropospheric and stratospheric processes on the vertical velocity within this part of the TTL. $\bar{\tau}_{360\,\mathrm{K}-400\,\mathrm{K}}$ gives 64 days, varying from 20 up to 90 days.

ACPD
9, 12597–12614, 2009

Fig. 2b displays the La Niña year 1998–1999. As might be expected, the overall shape is similar to the neutral ENSO year 2001–2002, with a right-skewed distribution. The maximum $\tau_{380\,\mathrm{K}-400\,\mathrm{K}}$ is shifted towards a longer residence time of 25 days, with the highest probability of 0.29, whereas $\tau_{360\,\mathrm{K}-380\,\mathrm{K}}$ is unevenly distributed and shifted towards shorter residence times of 10 to 15 days. Although the shape of the PDFs are slightly different to the ENSO neutral year 2001–2002, there is no change in $\bar{\tau}$. In contrast, the strong El Niño winter 1997–1998 (Fig. 2c) shows the clearest difference in the PDF distribution compared to the previous cases, with a symmetric distribution for all three theta layers. $\tau_{380\,\mathrm{K}-400\,\mathrm{K}}$ has two maximum bars at 25 and 30 days (0.3 and 0.23 probability), $\tau_{360\,\mathrm{K}-380\,\mathrm{K}}$ peaks at 35 days (0.13 probability) and $\tau_{360\,\mathrm{K}-400\,\mathrm{K}}$ shows a distinct maximum at 65 days with a high probability of 0.22. Although the PDFs have changed considerably compared to Fig. 2a and b, with a shift of the maxima to the right, only a slight increase of $\bar{\tau}$ is calculated. For this El Niño case, the maxima of $\tau_{360\,\mathrm{K}-380\,\mathrm{K}}$ and $\tau_{380\,\mathrm{K}-400\,\mathrm{K}}$ approximately sum up to the maximum of $\tau_{360\,\mathrm{K}-400\,\mathrm{K}}$, indicating that both layers have an influence on 360–400 K.

Concluding, during ENSO neutral and La Niña cases we find a right-skewed distribution for $\tau_{360\,\mathrm{K}-380\,\mathrm{K}}$ and $\tau_{380\,\mathrm{K}-400\,\mathrm{K}}$, whereas during El Niño the distribution is symmetric. A positive skew usually leads to a higher mean of the PDF due to the long right tail. Taking 380 K theta as the mean upper TTL layer, we can calculate the percentage of air parcels passing the TTL in less than 25 days. Almost 60% of the air needs less than 25 days travelling from 360 K to 380 K during ENSO neutral and La Niña years, whereas it accounts for less (48%) during El Niño years.

3.3 Interannual variability of residence time

The interannual variability of tropically averaged $\hat{\tau}$ is displayed in Fig. 3 for three different theta layers, covering the ERA40 and opECMWF time period from 1962–1963 until 2004–2005. $\hat{\tau}_{380\,\mathrm{K}-400\,\mathrm{K}}$ (red line) varies from a minimum of 31 days during 1986–87 up to 46 days during 1992–1993, displaying a higher variability than given by different ENSO events (Sect. 3.2). The average residence time is 38±5.1 days (2σ stan-

dard deviation). The time series of $\tau_{380\,K-400\,K}$ is highly correlated with $\tau_{LCP-400\,K}$ (not shown here). The corresponding $\hat{Q}_{380\,K-400\,K}$ varies from 0.48 K/day during 1992–1993 to 0.72 K/day during 1986–1987 with an average of 0.59 K/days (not shown here). $\hat{\tau}_{360\,K-380\,K}$ (blue line) varies from a minimum of 23 days during 1982–1983 up to 41 days during 1974–1975, with an average residence time of 34±7.3 days, faster than for the 380–400 K layer. There seems to be a negative trend for NH winter from 1962–1963 to 2001–2002, using the ERA40 time series. Inspecting $\hat{\tau}$ for the 360 K to 400 K theta layer (grey line), which is approximately the sum of $\hat{\tau}_{360\,K-380\,K}$ and $\hat{\tau}_{380\,K-400\,K}$, gives a residence time with an average of 70±7.6 days. Correspondingly, a negative trend also exists for the 360 K to 400 K layer, but not for the 380 K to 400 K layer. According to this, the time series of $\hat{\tau}_{360\,K-380\,K}$ has no correlation with $\hat{\tau}_{380\,K-400\,K}$ ($r=-0.14$), underlining the different characteristics of these two TTL layers (see Sect. 3.2). There is strong interannual variability, varying for $\hat{\tau}_{360\,K-400\,K}$ from maximum 76 days during 1973–1975 to minimum 60 days during 1982–1983. As expected, $\hat{Q}_{360\,K-400\,K}$ shows an increase from 1962–1963 to 2001–2002 and a high interannual variability, varying from a minimum of 0.54 K/days during 1973–1974 up to 0.73 K/day maximum during 1982–1983 (not shown here). This temporal behaviour of $\hat{\tau}$ and $\hat{Q}$ derived for the 360 K to 380 K theta layer seems to be connected with the reported trend of tropical tropopause height increase (Seidel and Randel, 2006), which is also visible by the increase of the LCP tropopause height over the time periods shown in Fig. 1. An increase of the tropical tropopause height within the 360 K to 380 K layer could be connected with a stronger tropospherically induced upwelling, and hence with a shorter residence time within this TTL layer. The distinct differences in $\hat{\tau}$ time series lead to the conclusion that the 380 K to 400 K theta layer must be dominated by stratospheric processes (the eddy-driven residual circulation), whereas the 360 K to 380 K layer reveals influences of tropospheric processes, which are accompanied by a positive trend of the tropical tropopause height. The question of whether a trend in τ and Q exists, or if it is a bias due to systematic changes in the ERA40 data assimilation procedure (Simmons et al., 2005), is discussed in more detail by K08. There is no distinct signal

ACPD
9, 12597–12614, 2009

of ENSO events or volcanic eruptions visible in the time series (Fig. 3), although these natural forcing events showed the largest impact on the LCP temperature and density distribution (K08). Thus, there have to be other or overlapping processes influencing the strong interannual variability of residence time in the TTL, which will be analysed in more detail in the next section.

3.4 Correlations with the Eliassen Palm-Flux

Tropical upwelling in the stratosphere is mainly driven by extratropical and equatorial waves (Randel et al., 2008). To address the influence of wave driving on the residence time in the TTL in more detail, we assess the correlation between τ and the Eliassen Palm (EP)-Flux, taking different pressure levels between 300 and 0.1 hPa from the ERA40 time period into account.

Figure 4a shows the maximum correlation between the vertical component of the EP-Flux (F_z), averaged between 45° and 75° S/N for SON/DJF at 150 hPa, and $\hat{\tau}_{360\,\mathrm{K}-400\,\mathrm{K}} \cdot F_z$ at 150 hPa (lowermost stratosphere) gives the amount of extratropical upward propagating planetary waves reaching stratospheric levels. F_z and $\hat{\tau}_{360\,\mathrm{K}-400\,\mathrm{K}}$ are anticorrelated with $r=-0.61$ at 99% significance. Intensified extratropical planetary wave propagation into the stratosphere generates enhanced extratropical wave driving, which is balanced by intensified diabatic upwelling in the tropics, hence leading to a shorter residence time in the TTL. There is one clear outlier in the scatter diagram at $15\,10^5$ kg/s^2 and 60 days, which is the NH winter 1982–1983. This is the first winter, following the El Chichon eruption in April 1982. However, no such deviation is visible for the NH winters 1963–1964 and 1991–1992, following the major volcanic eruptions of Mt. Agung (March 1963) and Mt. Pinatubo (June 1991). During the early 1980s, the ERA40 assimilation has a cold bias of 1 to 2 K (e.g. Fueglistaler and Haynes, 2005), which could lead to a stronger Q, hence shorter τ, impacting our analysis. Figure 4b reveals the maximum anticorrelation between the subtropical wave driving at 133 hPa and $\hat{\tau}_{360\,\mathrm{K}-400\,\mathrm{K}} \cdot$ A convergence of F (div$F<0$) in the stratosphere leads to a deceleration of the westerly flow and thus to a strengthening of the residual circulation on the winter hemisphere

side, the so called "wave driving" of the eddy driven residual circulation. We derive a strong anticorrelation of $r=-0.69$ (99% significant) between the subtropical wave driving and $\hat{\tau}_{360\,\mathrm{K}-400\,\mathrm{K}}$. Enhanced convergence in the subtropics leads to a shorter residence time between 360 K and 400 K. For $\hat{\tau}_{360\,\mathrm{K}-380\,\mathrm{K}}$ the anticorrelation maximizes even to $r\pm0.74$. Randel et al. (2008) found a strong convergence of the EP-Flux in the subtropical troposphere up to 100 hPa during NH and SH winter season due to extratropical and equatorial wave forcing. They also showed that this EP-Flux convergence is in balance with upwelling across the tropical tropopause. In accordance with this, we find that enhanced extratropical and subtropical wave driving leads to shorter $\hat{\tau}$ (stronger $\hat{Q}$) for the TTL between the 360 K to 400 K theta layers.

4 Conclusions

Concerning the interannual and spatial variability of residence time, the following new results are derived for NH winters from 1962–1963 to 2004–2005:

1. The residence time between the LCP and 400 K depends on the height of the LCP, which varies over time and location. In that respect a lower LCP tropopause corresponds with a longer residence time for the LCP and 400 K layer, but with a shorter residence time for the 360 K to LCP (~380 K) layer. This leads to the signature that $\tau_{\mathrm{LCP}-400\,\mathrm{K}}$ displays a spatially varying pattern, maximizing over the maritime continent, with the longest residence time found for the 1990s.

2. Zonally averaging the residence time for fixed theta layers gives a different meridional structure than that seen for the LCP to 400 K layers. For 380 K to 400 K, a shorter residence time (enhanced diabatic ascent) is found north of the Equator towards the winter hemisphere, which is probably due to the influence of enhanced extratropical wave driving. However, the residence time for the 360 K to 380 K and 360 K to 400 K layers has no defined meridional structure.

ACPD
9, 12597–12614, 2009

3. Averaging the residence time for the ERA40 DJF period from 1962–1963 to 2001–2002 gives a mean and 2σ standard deviation of 34±7.3 days for the 360 K to 380 K, 38±5.1 days for the 380 K to 400 K and 70±7.6 days for the 360 K to 400 K theta layers. The variance of tropically averaged τ amounts to ±40%, maximizing for the lower TTL between 360 K and 380 K.

4. Correlation analysis with the EP-Flux suggests that the high internannual variability of τ is caused by upward propagating extratropical planetary waves and by enhanced convergence in the subtropics in the lowermost stratosphere, during SH spring (SON) and NH (DJF) winter season. Enhanced extratropical and subtropical wave driving leads to a shorter residence time. Randel et al. (2008) first showed that this wave driving is in balance with upwelling across the tropical tropopause using an Eulerian approach and different vertical velocity fields.

5. The residence time of the lower part of the TTL ($\hat{\tau}_{360\,\mathrm{K}-380\,\mathrm{K}}$, $\hat{\tau}_{360\,\mathrm{K}-400\,\mathrm{K}}$) indicates a negative trend towards shorter residence times, which corresponds with the previously observed positive trend in the LCP tropopause height in the tropics. In contrast to this, the residence time for the 380 K to 400 K theta layers shows an increase during NH winters of the 1990s (ERA40), the period of weaker extratropical wave driving, reducing in the early 2000s (opECMWF).

6. Statistical analysing τ for different ENSO cases reveals a right-skewed distribution for ENSO neutral and La Niña and a symmetric distribution for El Niño years. Within 25 days ∼60% of air parcels travel through the 360 K to 380 K layers during the ENSO neutral winter 2001–2001 and the La Niña winter 1998–1999, whereas less air parcels (48%) reach 380 K during El Niño (1997–1998).

7. Of relevance for VSLS transport is the residence time between the 360–380 K theta layers, which has a minimum of less than 20 days over the tropical Western Pacific during the early 2000s period (not shown) coinciding with the maximum density of LCP trajectories.

ACPD
9, 12597–12614, 2009

There are distinct differences between the three considered theta layers leading to the conclusion, that the 380 K to 400 K layer is dominated by stratospheric influences, whereas the 360 K to 380 K layer shows more tropospheric influences. Our study illustrates the large spatial and interannual variability of residence time during NH winter season, which has to be considered in future TTL transport studies. Generally a decrease of residence time in the TTL leads to a faster supply and different ratios of VSL primary and secondary source gases transported into the stratosphere. In that respect a negative trend in residence time in a future climate could have a significant influence on the stratospheric ozone layer as the chlorine loading is expected to relax to pre-industrial levels.

Acknowledgements. We would like to thank the ECMWF for providing the meteorological analyses and the technical data support. The authors thank the editor Rob MacKenzie for his useful recommendations, which helped to improve this manuscript. This study was partly funded by the European Union's 6th framework program within the SCOUT-O_3 (GOCE-CT-2004-505390) project.

References

Bonazzola, M. and Haynes, P.: A trajectory-based study of the tropical tropopause region, J. Geophys. Res., 109(D20), 112, doi:10.1029/2003JD004356, 2004. 12603

Dunkerton, T.: On the mean meridional mass motions of the stratosphere and mesosphere, J. Atmos. Sci., 35, 2325-2333, 1978. 12599

Fueglistaler, S. and Haynes, P.: Control of interannual and longer-term variability of stratospheric water vapor, J. Geophys. Res., 110, D24108, doi:10.1029/2005JD006019, 2005. 12603, 12606

Fueglistaler, S., Wernli, H., and Peter, T.: Stratospheric water vapor predicted from the Lagrangian temperature history of air entering the stratosphere in the tropics, J. Geophys. Res., 110, D03108, doi:10.1029/2003JD004069, 2004.

Haynes, P., Marks, C., McIntyre, M., Shepherd, T., and Shine, K.: On the "Downward Control" of extratropical diabatic circulations by eddy-induced zonal mean forces, J. Atmos. Sci., 49, 651–679, 1991. 12599

Holton, J. and Gettelman, A.: Horizontal transport and the dehydration of the stratosphere, Geophys. Res. Lett., 28, 2799–2802, 2001. 12599

Immler, F., Krüger, K., Tegtmeier, S., Fujiwara, M., Fortuin, P., Verver, Gé, and Schrems, O.: Cirrus clouds, humidity, and dehydration in the tropical tropopause layer observed at Paramaribo, Suriname (5.8° N, 55.2° W), J. Geophys. Res., 112, D03209, doi:10.1029/2006JD007440, 2007. 12600

Krüger, K., Tegtmeier, S., and Rex, M.: Long-term climatology of air mass transport through the Tropical Tropopause Layer (TTL) during NH winter, Atmos. Chem. Phys., 8, 813–823, 2008, http://www.atmos-chem-phys.net/8/813/2008/. 12599

Marcy, T. P., Popp, P. J., Gao, R. S., et al.: Measurements of trace gases in the tropical tropopause layer, Atmos. Environ., 41, 7253–7261, 2007. 12599

Park, S., Jiménez, R., Daube, B. C., Pfister, L., Conway, T. J., Gottlieb, E. W., Chow, V. Y., Curran, D. J., Matross, D. M., Bright, A., Atlas, E. L., Bui, T. P., Gao, R.-S., Twohy, C. H., and Wofsy, S. C.: The CO_2 tracer clock for the Tropical Tropopause Layer, Atmos. Chem. Phys., 7, 3989–4000, 2007, http://www.atmos-chem-phys.net/7/3989/2007/. 12599

Pawson, S. and Naujokat, B.: The cold winters of the middle 1990s in the northern lower stratosphere, J. Geophys. Res., 104, 14 209-14 222, 1999. 12602

Quack, B. and Wallace, D.: Air-sea flux of bromoform: Controls, rates, and implications, Global Biogeochem. Cy., 17, 1023, doi:10.1029/2002GB001890, 2003. 12599

Randel, W., Garcia, R., and Wu, F.: Dynamical Balances and Tropical Stratospheric Upwelling, J. Atmos. Sci., 65, 3584–3595, 2008. 12606, 12607, 12608

Seidel, D. and Randel, W.: Variability and trends in the global tropopause estimated from radiosonde data, J. Geophys. Res., 111, D21101, doi:10.1029/2006JD007363, 2006. 12605

Simmons, A., Hortal, M., Kelly, G., McNally, A., Untch, A., and Uppala, S.: ECMWF Analyses and Forecasts of Stratospheric Winter Polar Vortex Breakup: September 2002 in the Southern Hemisphere and Related Events, J. Atmos. Sci., 62(3), 668–689, 2005. 12600, 12605

Tegtmeier, S., Rex, M., Krüger, K., Wohltmann, I., and Schoellhammer, K.: Variations of the residual circulation in the northern hemispheric winter, J. Geophys. Res., 113, D16109, doi:10.1029/2007JD009518, 2008. 12600

Uppala, S., Kållberg, P. W., Simmons, A. J., et al.: The ERA-40 Re-analysis, Q. J. Roy. Meteor. Soc., 131(612), 2961-3012, 2005. 12600

World Meteorological Organization: Scientific Assessment of Ozone Depletion: 2006, WMO Global Ozone Research and Monitoring Project, Report No. 50, 2007. 12598, 12599

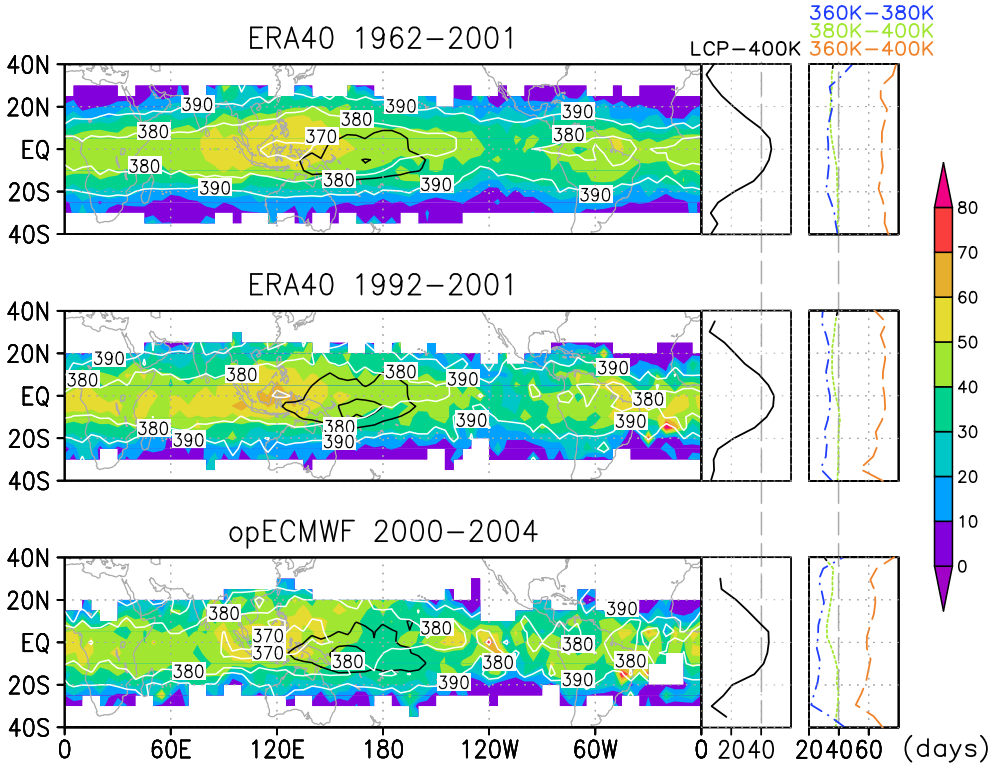

Fig. 1. DJF long-term climatology; Left: $\tau_{\mathrm{LCP-400\,K}}$ [days] (color shading), Θ [K] and density of LCPs (white and black contours); Right: Zonal mean τ[days] for LCP–400 K (black line), 380 K–400 K (green line), 360 K–380 K (blue line) and 360 K–400 K (orange line). Top panel: 1962/1963–2001/2002 ERA40 data; middle panel: 1992/1993–2001/2002 ERA40 data; lower panel: opECMWF data from 2000/2001–2004/2005. Contour intervals for the trajectory density are 0.005 and 0.01 per 5°×5° grid.

ACPD
9, 12597–12614, 2009

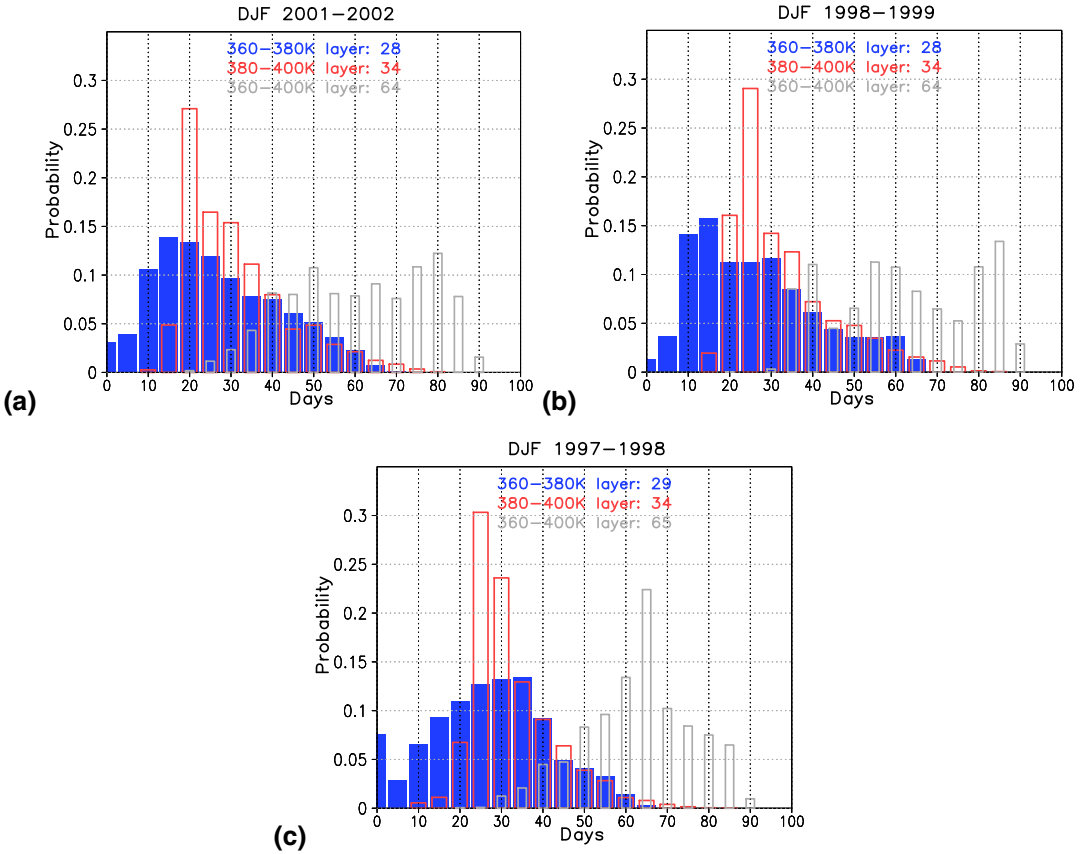

Fig. 2. PDF of $\tau_{380\,\mathrm{K}-400\,\mathrm{K}}$ (red bars), $\tau_{360\,\mathrm{K}-380\,\mathrm{K}}$ (blue filled bars) and $\tau_{360\,\mathrm{K}-400\,\mathrm{K}}$ (grey bars) for DJF trajectories of: **(a)** ENSO neutral winter 2001–02, **(b)** La Niña winter 1998–1999 and **(c)** El Niño winter 1997–1998; given in [days] taking 5 K centered theta bins into account. The coloured numbers give the corresponding winter average of τ.

ACPD
9, 12597–12614, 2009

Title Page
Abstract Introduction
Conclusions References
Tables Figures
◀I ▶I
◀ ▶
Back Close
Full Screen / Esc
Printer-friendly Version
Interactive Discussion

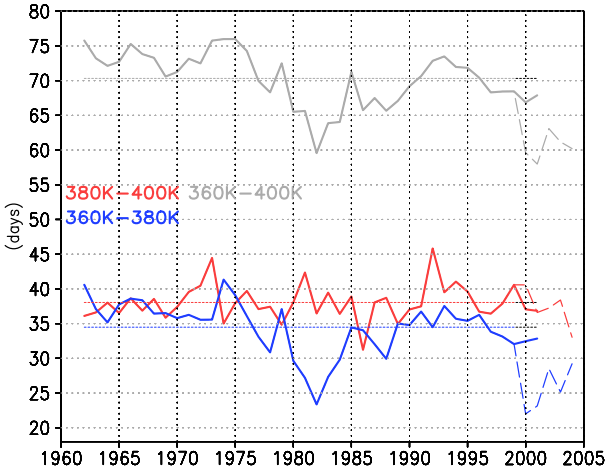

Fig. 3. Interannual variability of $\hat{\tau}_{380\,\mathrm{K}-400\,\mathrm{K}}$ (red line), $\hat{\tau}_{360\,\mathrm{K}-380\,\mathrm{K}}$ (blue line) and $\hat{\tau}_{360\,\mathrm{K}-400\,\mathrm{K}}$ (grey line) from 1962–1963/2004–2005. $\hat{\tau}$ is calculated from Fig. 1. The short dashed lines give the long-term mean of τ. The solid/long dashed lines display ERA40/opECMWF data.

ACPD

9, 12597–12614, 2009

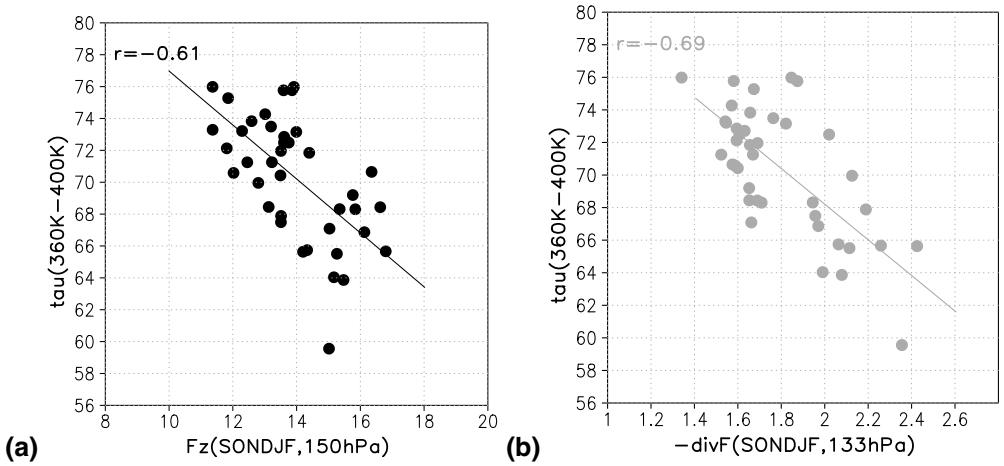

Fig. 4. Scatter plots and correlation coefficients between: **(a)** F_z [10^5 kg/s^2] at 150 hPa and $\hat{\tau}_{380\,\mathrm{K}-400\,\mathrm{K}}$ [days]; **(b)** −div$F$ [m/s/d] at 133 hPa and $\hat{\tau}_{360\,\mathrm{K}-400\,\mathrm{K}}$ [days]. The EP-Flux components are averaged for: **(a)** SON/DJF 45–75° S/45–75° N; **(b)** SON/DJF 10–20° S/ 10–20° N using ERA40 data.

ACPD
9, 12597–12614, 2009